

**Insight into the Excited State Electronic and Structural Properties of the Organic Photovoltaic Electron Donor Polymer Poly(thieno[3,4-b]thiophene benzodithiophene) by Means of *ab Initio* and Density Functional Theory**

Itamar Borges, Jr,<sup>§,†,¶,\*</sup> Elmar Uhl,<sup>¶</sup> Lucas Modesto-Costa,<sup>†</sup> Adélia A. J. Aquino,<sup>§</sup> and Hans Lischka<sup>§,°,\*</sup>

<sup>§</sup>Department of Chemistry and Biochemistry, Texas Tech University, Lubbock, Texas 79409-1061, USA

<sup>†</sup> Departamento de Química, Instituto Militar de Engenharia, Praça General Tibúrcio, 80, 22290-270 Rio de Janeiro, Brazil

<sup>¶</sup> Programa de Pós-Graduação em Engenharia de Defesa, Instituto Militar de Engenharia, Praça General Tibúrcio, 80, 22290-270 Rio de Janeiro, Brazil

<sup>°</sup> Institute for Theoretical Chemistry, University of Vienna, 1090 Vienna, Austria

\* [itamar@ime.eb.br](mailto:itamar@ime.eb.br); [hans.lischka@univie.ac.at](mailto:hans.lischka@univie.ac.at)

## Table of Contents:

<b>Figure S1:</b> Testing of orbital freezing schemes	p. S3
<b>Figure S2:</b> PTB1 ( $n=1-3$ ) ADC(2) excitation energies as function of the type of basis set using the SV-SVP/PBE optimized geometry for each oligomer	p. S4
<b>Figure S3:</b> Computed carbon-sulfur bond distances	p. S5
<b>Figure S4:</b> Computed single carbon-carbon bond distances	p. S6
<b>Figure S5:</b> Computed double carbon-carbon bond distances	p. S7
<b>Figure S6:</b> (PTB1) <sub>5</sub> $\Omega_{AB}^{\alpha}$ plots of the first four electronic transitions ( $S_1$ to $S_4$ ) employing ADC(2), B3LYP and the SV-SVP basis set	p. S8
<b>Figure S7:</b> (PTB1) <sub>4</sub> ground ( $S_0$ ) and excited ( $S_1$ ) optimized geometries	p. S9
<b>Table S1:</b> (PTB1) <sub>1</sub> excitation character and transition energy $\Delta E$ in eV using the SV-SVP, SVP, TZVP and TZVP-def2-S' basis sets and default freezing	p. S10
<b>Table S2:</b> (PTB1) <sub>2</sub> excitation character and transition energy $\Delta E$ in eV using the SV-SVP, SVP, TZVP and TZVP-def2-S' basis sets and default freezing.	p. S11
<b>Table S3:</b> (PTB1) <sub>3</sub> excitation character and transition energy $\Delta E$ in eV using the SV-SVP, SVP, TZVP and TZVP-def2-S' basis sets	p. S12

## Testing of the freezing scheme

In testing the freezing of occupied and molecular orbitals, the (PTB1)<sub>1</sub> S<sub>1</sub> transition energy was computed systematically using the 18 freezing schemes depicted in Figure S1 below. The results show for a given percentage of frozen occupied orbitals in the range from 70% to 90% that increasing the percentage of frozen virtual orbitals up to 50% increases the S<sub>1</sub> transition energies of (PTB1)<sub>1</sub> by at most ~ 0.2 eV. In total, the S<sub>1</sub> excitation energy increases only by less than 0.4 eV over the whole range of freezing schemes. This quite modest dependence of the excitation energies in the range of our freezing schemes lets us expect that the overall error in the computed transition energies of (PTB1)<sub>5</sub> using the 60% frozen occupied and 50% frozen virtual scheme should not exceed 0.3 to 0.4 eV.

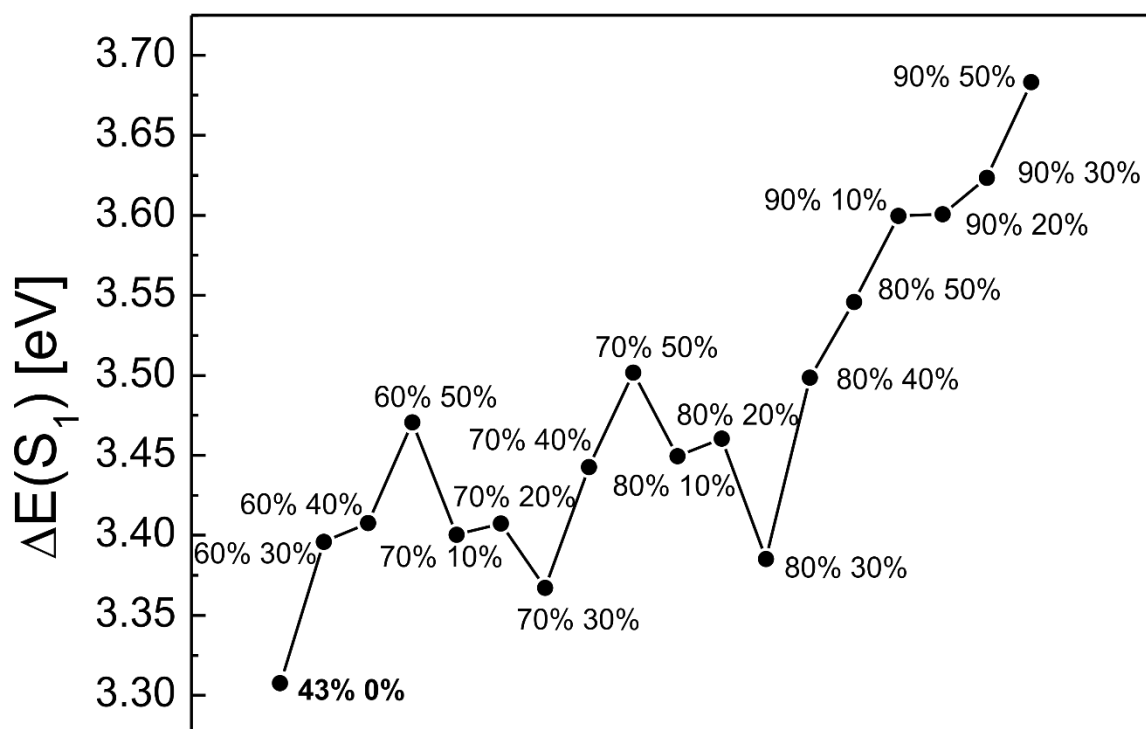


**Figure S1.** ADC(2)/SV-SVP testing of freezing schemes for the first excitation energy  $\Delta E(S_1)$  of (PTB1)<sub>1</sub>. Notation for each pair of percentage is: first number - percentage of lowest energy frozen occupied orbitals (%); second number - percentage of highest energy frozen virtual orbitals (%). For (PTB1)<sub>1</sub> the freezing of only the core orbitals (standard freezing) corresponds to (43%, 0 %).

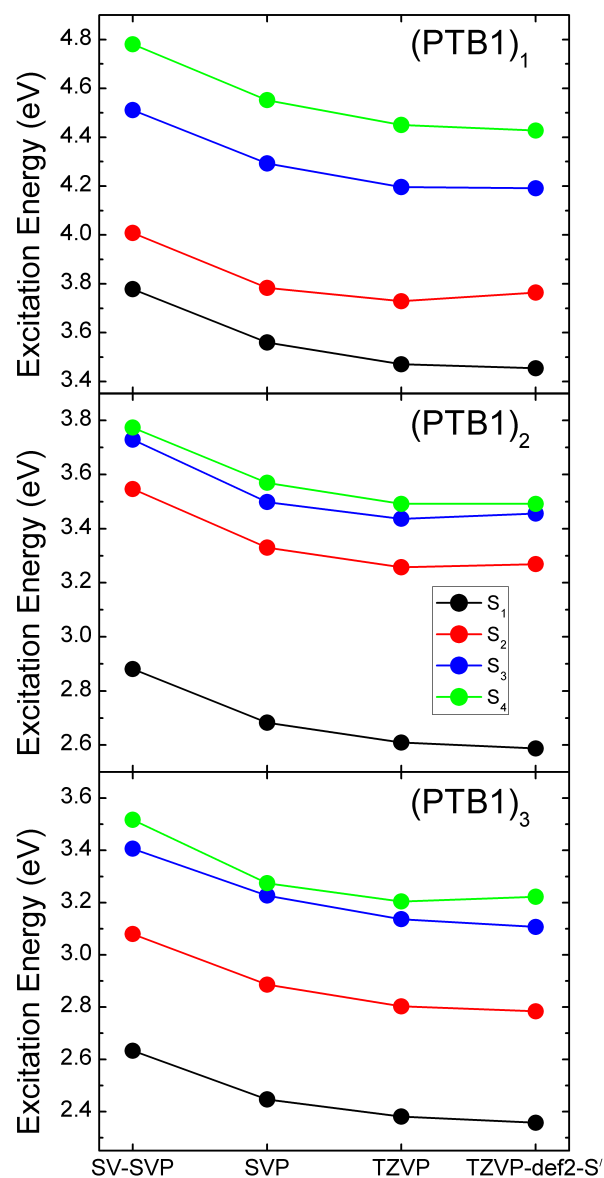


**Figure S2.** PTB1 ( $n=1-3$ ) ADC(2) excitation energies  $\Delta E$  (eV) as function of the type of basis set using the SV-SVP/PBE optimized geometry for each oligomer. TZVP-def2-S' contains the TZVP basis set for the C and H atoms and the def2-TZVP basis set for sulfur, which includes polarization functions (2d/1f).

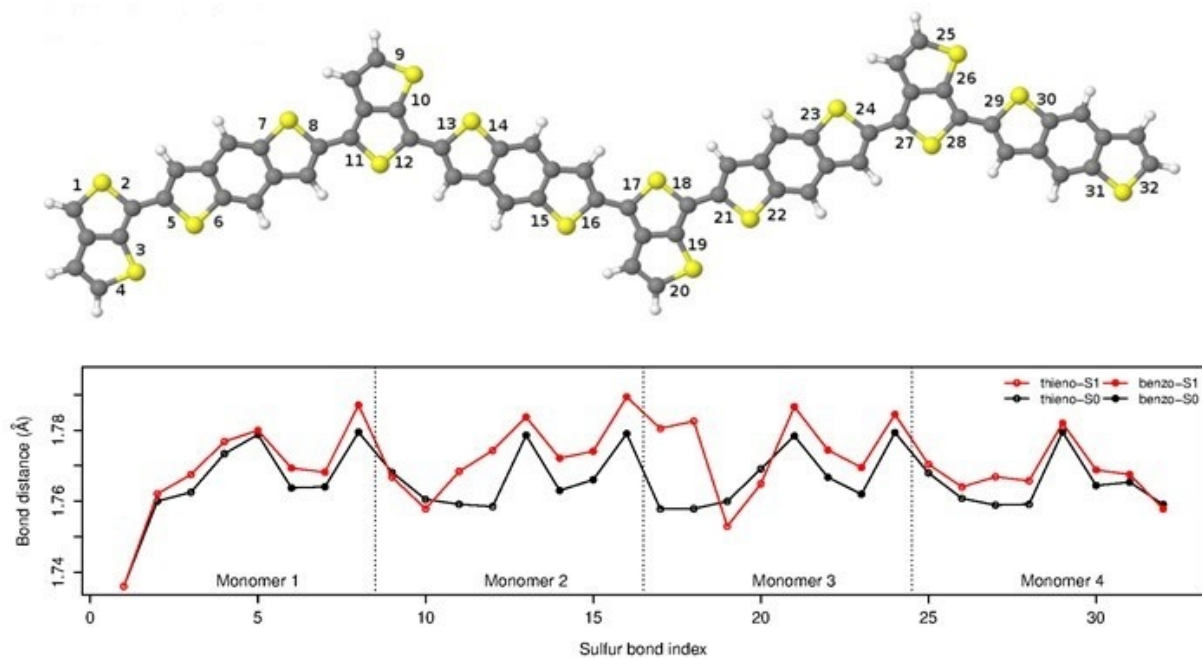


**Figure S3.** Computed carbon-sulfur bond distances for the optimized structures of the  $S_0$  and  $S_1$  states of the PTB1 tetramer using the MP2 and ADC(2)/SV-SVP methods.

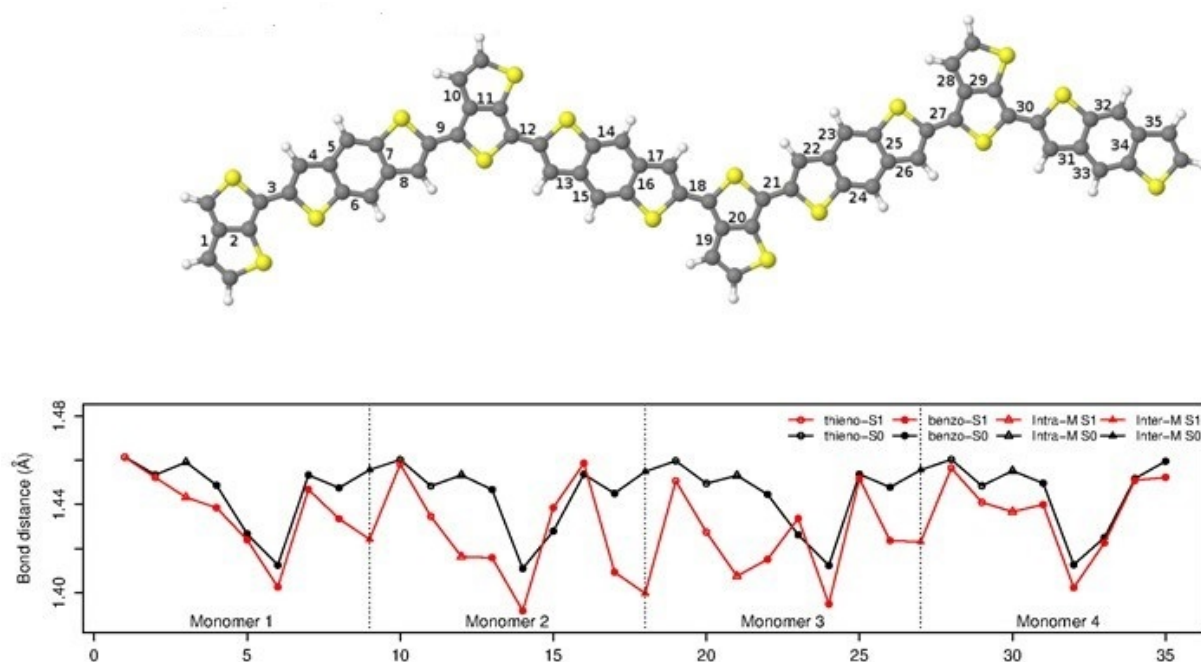


**Figure S4.** Computed single carbon-carbon bond distances for the optimized structures of the  $S_0$  and  $S_1$  states of the PTB1 tetramer using the MP2 and ADC(2)/SV-SVP methods.

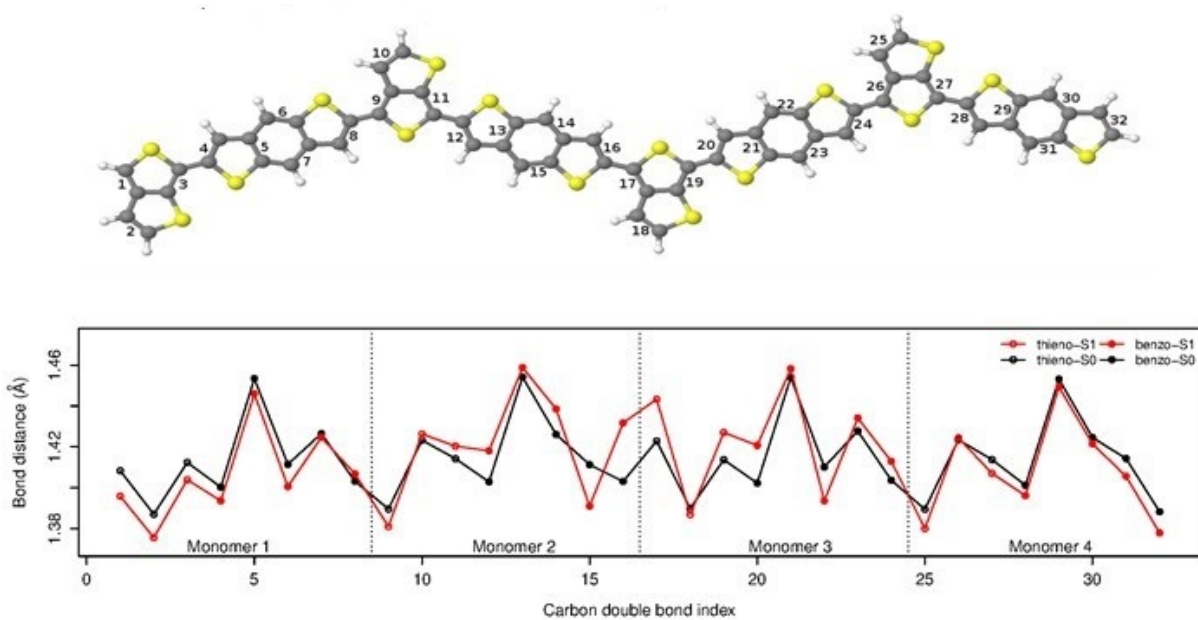


**Figure S5:** Computed double carbon-carbon bond distances for the optimized structures of the  $S_0$  and  $S_1$  states of the PTB1 tetramer using the MP2 and ADC(2)/SV-SVP methods.

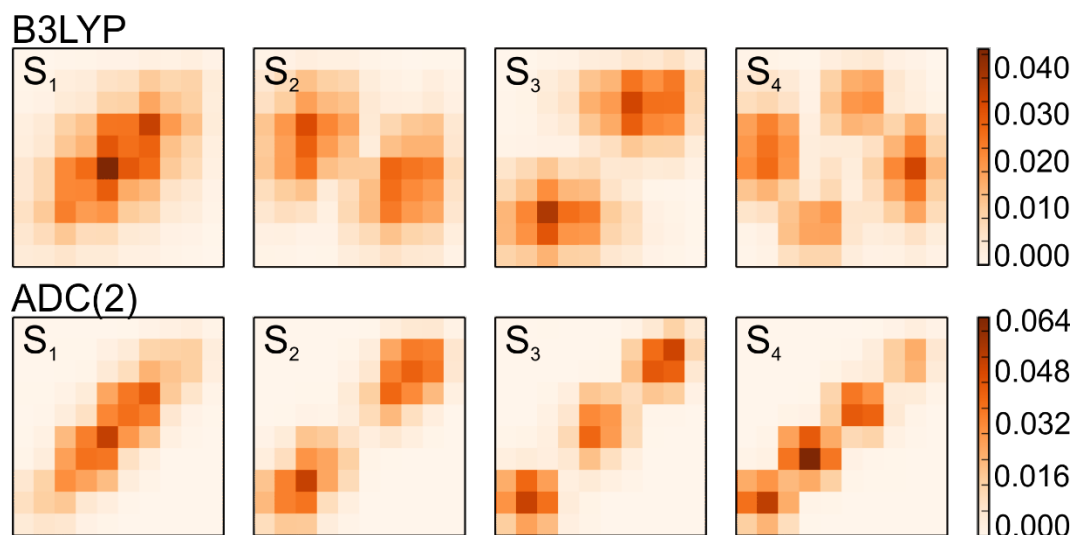


**Figure S6:**  $(\text{PTB1})_5 \Omega_{AB}^\alpha$  plots of the first four electronic transitions ( $S_1$  to  $S_4$ ) employing ADC(2), B3LYP and the SV-SVP basis set. The vertical axis indicates the position of the hole and the horizontal axis the position of the electron. Each square of the plot represents either a benzodithiophene or a thienothiophene subunit. The square in the lowest leftmost corner corresponds to the electron rich benzodithiophene moiety and in the highest rightmost corner to the electron deficient thienothiophene. The shades represent the probability values according to the scale on the right of each panel.



**Figure S7:** (PTB1)<sub>4</sub> ground ( $S_0$ ) and excited ( $S_1$ ) optimized geometries using the SV-SVP basis set.

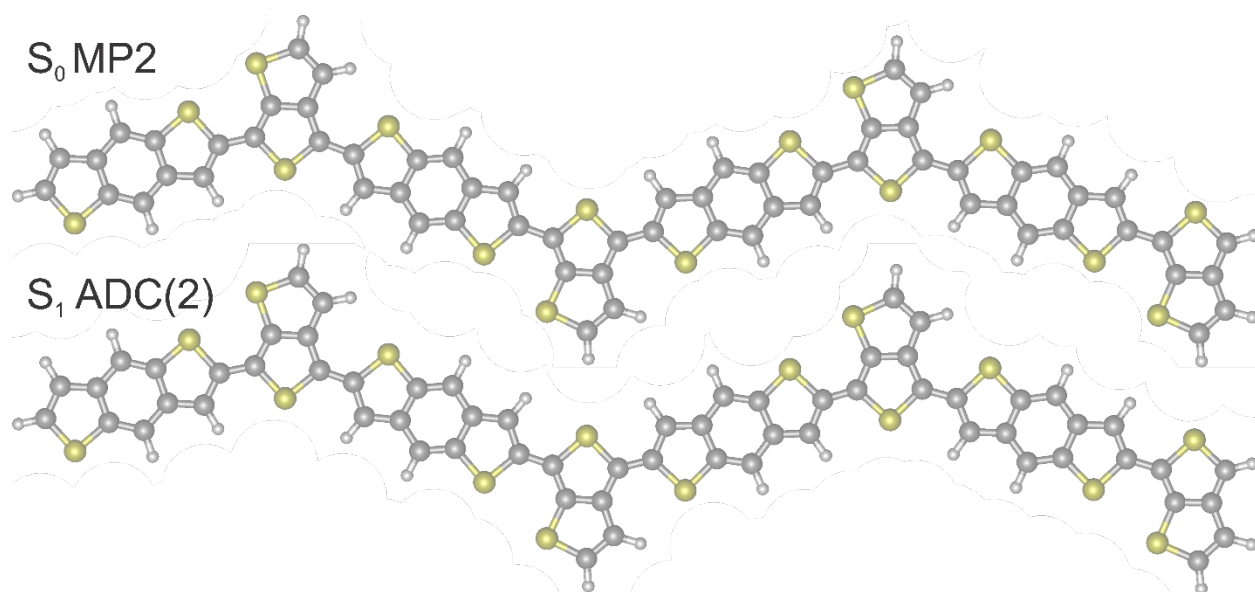


**Table S1.** (PTB1)<sub>1</sub> excitation character and transition energy  $\Delta E$  (eV) using the SV-SVP, SVP, TZVP and TZVP-def2-S' basis sets and standard freezing.

State	Character % (SV-SVP/SVP/TZVP/ TZVP-def2-S')
$S_1-2^1A'$	(93.6/91.8/92.0/93.5)(HOMO $\rightarrow$ LUMO)
$S_2-3^1A'$	(64.6/72.1/70.8/68.5)(HOMO-1 $\rightarrow$ LUMO)
$S_3-4^1A'$	(48.0/47.3/50.2/55.3)(HOMO $\rightarrow$ LUMO+1)
$S_4-5^1A'$	(33.7/37.9/31.5/32.5)(HOMO-2 $\rightarrow$ LUMO) + (26.5/27.9/30.9/29.8)(HOMO $\rightarrow$ LUMO+2)

State	$\Delta E$ (SV-SVP)	$\Delta E$ (SVP)	$\Delta E$ (TZVP)	$\Delta E$ (TZVP-def2-S')
$S_1-2^1A'$	3.779	3.559	3.471	3.454
$S_2-3^1A'$	4.008	3.783	3.728	3.764
$S_3-4^1A'$	4.511	4.292	4.197	4.191
$S_4-5^1A'$	4.781	4.552	4.450	4.427

**Table S2.** (PTB1)<sub>2</sub> excitation character and transition energy  $\Delta E$  (eV) using the SV-SVP, SVP, TZVP and TZVP-def2-S' basis sets and standard freezing.

State	Character % (SV-SVP/SVP/TZVP/ TZVP-def2-S')
$S_1-2^1A'$	(92.9/91.9/91.9/92.8)(HOMO $\rightarrow$ LUMO)
$S_2-3^1A'$	(65.9/56.5/61.6/69.7)(HOMO-1 $\rightarrow$ LUMO)
$S_3-4^1A'$	(51.2/48.0/52.7/34.7)(HOMO-3 $\rightarrow$ LUMO)
$S_4-5^1A'$	(68.2/28.1/37.0/24.9)(HOMO $\rightarrow$ LUMO+1)+(8.4/35.5/31.1/16.4)(HOMO-2 $\rightarrow$ LUMO)

State	$\Delta E$ (SV-SVP)	$\Delta E$ (SVP)	$\Delta E$ (TZVP)	$\Delta E$ (TZVP-def2-S')
$S_1-2^1A'$	2.881	2.683	2.609	2.588
$S_2-3^1A'$	3.546	3.330	3.257	3.269
$S_3-4^1A'$	3.729	3.498	3.437	3.456
$S_4-5^1A'$	3.773	3.570	3.491	3.491

**Table S3.** (PTB1)<sub>3</sub> excitation character and transition energy  $\Delta E$  (eV) using the SV-SVP, SVP, TZVP and TZVP-def2-S' basis sets and standard freezing.

State	Character % (SV-SVP/SVP/TZVP/ TZVP-def2-S')
$S_1-2^1A'$	(83.9/83.6/83.8/84.7)(HOMO $\rightarrow$ LUMO)
$S_2-3^1A'$	(45.7/46.4/45.0/44.4)(HOMO-1 $\rightarrow$ LUMO)+(44.1/42.6/44.2/45.9)(HOMO $\rightarrow$ LUMO+1)
$S_3-4^1A'$	(33.7/29.5/33.2/36.1)(HOMO-1 $\rightarrow$ LUMO)+(36.2/32.3/34.4/35.8)(HOMO $\rightarrow$ LUMO+1)
$S_4-5^1A'$	(38.0/28.9/34.3/40.8)(HOMO-2 $\rightarrow$ LUMO)+(19.5/22.4/20.4/14.6)(HOMO-4 $\rightarrow$ LUMO)

State	$\Delta E$ (SV-SVP)	$\Delta E$ (SVP)	$\Delta E$ (TZVP)	$\Delta E$ (TZVP-def2-S')
$S_1-2^1A'$	2.633	2.446	2.380	2.357
$S_2-3^1A'$	3.080	2.885	2.803	2.783
$S_3-4^1A'$	3.407	3.227	3.137	3.107
$S_4-5^1A'$	3.517	3.274	3.205	3.222